12-1-2016

Computational analysis in vivo p53 binding sites in the context of chromatin and repeat regions

Feifei Bao

Computational analysis in vivo p53 binding sites in the context of chromatin and repeat regions

By

Feifei Bao

A thesis submitted in partial fulfillment of the requirements for the degree of Master of Science in Bioinformatics at the Rochester Institute of Technology

R·I·T

Bioinformatics Program
Thomas H. Gosnell School of Life Sciences
College of Science
Rochester Institute of Technology
Rochester, NY

1 December 2016

Committee Signatures

The undersigned state that Feifei Bao, a candidate for the Master of Science degree in Bioinformatics, has submitted her thesis and has satisfactorily defended it.

This completes the requirements for the Master of Science degree in Bioinformatics at Rochester Institute of Technology.

Feng Cui, Ph.D. Date
Adviser

Gary R. Skuse, Ph.D. Date
Committee Member

Gregory Babbitt, Ph.D. Date
Committee Member

Table of Contents

List of Figures

Acknowledgements

I would first like to thank my thesis advisor Prof. Feng Cui of the College of Science at Rochester Institute of Technology for the support of my MS study and research, for his patience, encouragement, enthusiasm and immense knowledge. It has been an honor to work with him.

Besides my advisor, I would also like to thank the rest of my thesis committee members: Prof. Gary R. Skuse and Prof. Gregory Babbitt for their interest in my work and insightful comments.

In addition, I would like to thank my fellows: Nick, Tom, Julia, Denisse and Anogna for their help in my study and research. We were working together and have had a great time.

The most special thanks goes to my parents. They give me unconditional support and love during my time here. Finally, there are my friends. We were not only able to support and encourage each other but also made a lot of fun.

Abstract

The p53 tumor suppressor protein is involved in multiple central cellular processes and human cancer occurrences. A research effort is proposed to collect the majority of p53 ChIP fragments up to now and reveal the binding pattern of p53 binding sites. It demonstrates that the normal and cancer cell lines have significantly different chromatin organizations around P53 binding sites. Based on the high occurrences, the core binding sites can be collected to analyze gene expression configurations. Depending on the accessibility of p53 sites and epigenetic marks in the chromatin context, p53 binds to its target sites in repetitive regions. Finally, the functional annotation analysis illustrates that the most enriched pathway of p53 ChIP fragments is p53 signaling pathway and highly enriched clusters relating to apoptosis, DNA damage and cellular signaling are modulated by p53.

Introduction

Biological Background

The human genome contains approximately 3 billion base pairs of DNA packaged into 23 chromosomes. Each cell has two copies of genetic information. There are about 50 trillion cells, tens of thousands of individual proteins and genes, in typical human body. The Central Dogma of Molecular Biology reveals the genetic inheritance and specification: replication of DNA, transcription into mRNA and translation into protein.

The large amount of genetic information is arranged into a structure called chromatin. Chromatin is composed of a combination of DNA, histones and certain types of RNA. The basic, repeated structure unit of chromatin is the nucleosome. Histones are alkaline, positively charged proteins, which include 4 core histones, namely H2A, H2B, H3, and H4. H2A and H2B residing in core domain keep from organize to nucleosomes. H3 and H4 locating in the side of the structure bind to the DNA to regulate chromatin formation [1]. H1 and H5 are the linker histones. They bind with nucleosome core and linker DNA [2]. A strand of 145bp DNA wraps in 1.6 turns around the core histones (Figure 1) [3].

Figure 1. Nucleosomal DNA wraps around histones

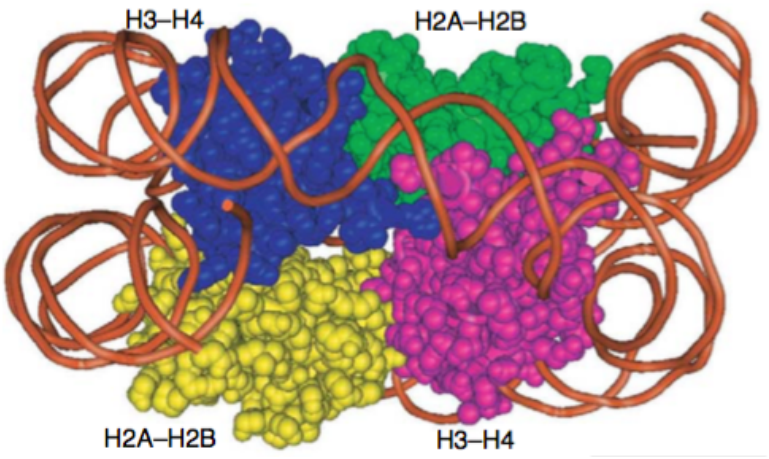

The ability of interaction between Transcriptional Factors (TFs) and their cognate

sites will be weakened, given the DNA sequence occluded by nucleosomes. Two main factors have been identified to be able to regulate the function state of chromatin. One is the methylated DNA and the other is modified histone protein [4]. While the DNA methylation can be found in most CpGs area of the genome [5], the histone modification occurs more widely within the amino-terminal histone tails relating with various biological functions.

A protein should contact with histones or nucleosomal DNA to interact with a nucleosome. The target sites cannot access protein successfully if its nucleosome is wrapped tightly. Several researchers show that some specific proteins can bind to DNA sequences directly (hereafter "nucleosome DNA-binding proteins") in vitro and in vivo, such as telomeric protein Rap1p [6], yeast chromatin-remodeling complexes SWI/SNF, RSC [7] and so on. The modification of Nucleosome-Interacting Proteins can influence the DNA binding to TFs.

DNA Binding Protein - P53

In this study, we focus on the best-known tumor suppressor protein p53, which works as a sequence-specific transcription factor. P53 with a high-resolution crystal structures plays an important role in various central cellular processes, such as the maintenance of genetic stability, cell cycle control, transcription, DNA repair, apoptosis and other responses [8]. In most cases of human cancers, p53 mutates is functionally inactivated by signal-dependent modifications, since the central conserved region of p53 is necessary and important for specific DNA binding [9]. When the cell is normal and unstressed, the short-lived p53 protein level can keep a low turnover and latent state. However when p53 is activated due to some genotoxic stresses like DNA damage, nucleotide depletion and hypoxia, p53 will accumulate and work as a transcription factor. The activation can inhibit many gene expressions and induce some responses like cell cycle arrest or apoptosis [10].

Kaeser and Lggo [11] proposed some models to explain why p53 causes cell cycle arrest in some places and apoptosis in others. The reason is that p53 binds with high affinity to the response elements regulating cell cycle arrest genes (CCA-sites)

and binds to the promoters of apoptosis (Apo-sites) – inducing genes with a lower affinity. The evidence is that some low-affinity mutants keep the ability to induce cell cycle arrest.

The Structure of P53

The DNA-binding protein P53 looks like a self-assembled tetramer [11]. It contains two copies of a decamer motif "RRRCWWGYYY"(R=A, G; W=A, T; Y=C, T) separated by a variable spacer of 0 to 13 base pairs (Figure 2).

Figure 2. Four p53 core domains bound to bent DNA.

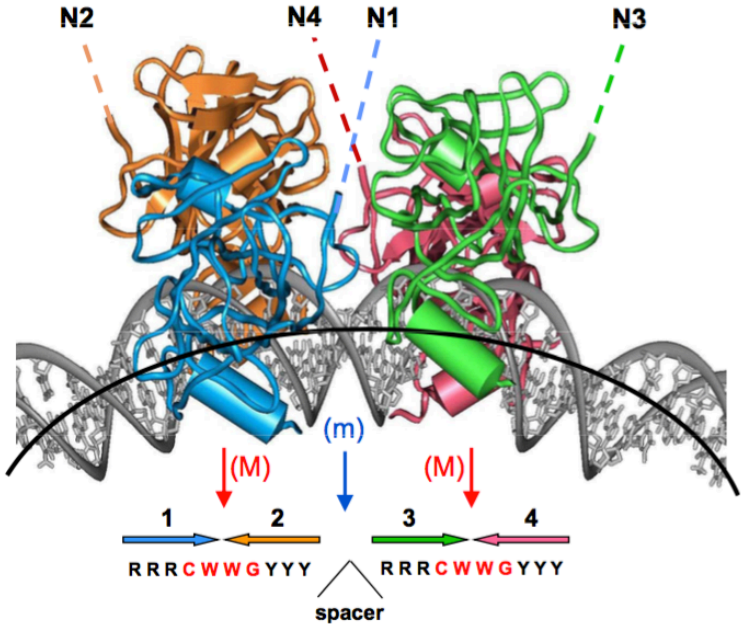

P53 has four molecules of DNA binding domain (p53DBD) [12]. More than 80% missense mutations happen in p53DBD, which leads to DNA binding disrupture or stability reduction [11]. These four p53 motifs are positioned on the external side of the DNA loop and recognize their cognate sites in nucleosome DNA if the p53 sites are exposed (Figure 2). P53DBD bends the DNA to improve the stability and cooperation of binding.

Figure 3. Modeling of p53 tetramer bound to nucleosome DNA.

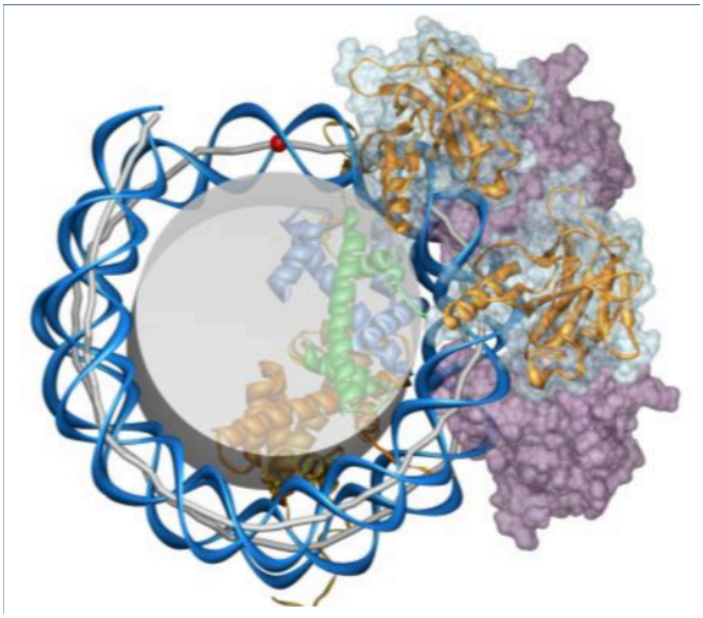

Sahu and Wang [13] reported the idea that when the p53 binding sites are bent in the same direction with DNA complexes in solution and in co-crystals, the sites have high accessibility. However, if the direction of p53 binding sites in the core particle are turned ~ 180 degrees, they become inaccessible. That means they are in the opposite directions and statuses. Figure 3 shows that when the p53 binding sites are exposed on the nucleosome surface, they are recognized by corresponding p53. Therefore, the direction and position of the p53 binding sites determine whether or not they can be contacted easily. When the p53 site is "exposed" to the surface, it is accessible to p53. By contrary, it is inaccessible if the site is "buried".

Thesis Goals

In this study, we collected the most comprehensive p53 ChIP fragments to compare the normal and cancer cell lines. Clusters with overlapping p53 ChIP fragments will be analyzed in terms of their distances to the transcription start site (TSS) of nearest genes. We hypothesize that there is a significant difference in the distances between the normal and cancer p53 clusters. Using statistic analyses, we can test this hypothesis.

Some researchers reported that various p53 binding sites have been identified in

sequences of primate-specific interspersed repeats. Around 1509 of ≈319, 000 human ERV LTR regions have a near-perfect p53 DNA binding site [14]. Zemojtel et al. [15] reported that about 15 percentages of in vivo p53 sites could be derived in the short interspersed nuclear element (SINE). Harris et al. [16] also detected that a large number of p53 DNA binding sites in long interspersed nuclear elements-1 (L1s) within the human genome. All these p53 binding sites reside in the 19 primate-specific Alu elements (SINE). Therefore, we plan to detect all the p53 binding sites up to now residing in repetitive regions and investigate their distributions. The Gudkov's group has shown that p53 cooperates with DNA methylation to maintain epigenetic silencing of repeats, which include major classes of short, interspersed nuclear elements (SINE) B1 and B2 [17]. Thus we will analyze all the collection of p53 ChIP fragments to see how they are distributed among repetitive regions. Furthermore, based on the observations of these clusters, we can reveal their highly enriched pathways and clusters to do p53 functional analysis.

Methods and Materials

Collection of P53 Binding Sites

Generally, there are two main different ways to identify p53 binding sites (BSs). The first traditional approach [18] focuses on a specific p53 response element (RE), which can be regulated by p53 protein. It demonstrates the p53 RE by test gene regulation and chromatin immunoprecipitation with a p53-specific antibody. The second approach is high-throughput sequencing of chromatin immunoprecipitated DNA (ChIP-seq), which can map the in vivo genome-wide binding sites of DNA-binding proteins [19]. The extractions of the p53-bound DNA fragments by chromatin immunoprecipitation (ChIP) are denoted ChIP fragments below.

For better analysis, we translated all the p53 ChIP fragments into the same assembly hg18 by UCSC genome browser liftOver utility (https://genome.ucsc.edu/cgi-bin/hgLiftOver). Based on the cell type, they were

separated into two datasets: cancer p53 ChIP fragments and normal p53 ChIP fragments.

Concordance Between P53 Binding Sites Identified in Vitro and in Vivo

Besides the collected ChIP segments identified in vivo, a list of known 154 famous p53 REs [18] were studies to validate the assumption that the p53 ChIP fragments can show the strong evidence of REs. Riley et al. [18] proposed that to identify p53 – regulated genes, several criteria should be executed. P53 REs near or in the gene could regulate the test gene and be regulated by activated wild p53 protein. Most REs contains two half sequencing sites separated by a variable length spacer.

Once the ChIP fragments and REs are prepared, the sequence data and annotations can be visualized using UCSC Genome Browser (https://genome.ucsc.edu). Import the normal datasets and cancer datasets as annotations tracks with assembly hg18 in Genome Brower. Then locate the p53 REs in UCSC Genome Browser based on their genome positions to focus on the specific areas. Therefore, we can have an overview of the p53 REs distributions in p53 ChIP fragments.

Detection of P53 Core Binding Sites

Many binding sites were shared by most of the experiments/treatments, like 5-FU, Nutlin 3a. After mapping all the p53 binding sites to the human genome (hg18), there are many overlapping areas in every human chromosome. So along the chromosome, every fragment has the occurrence based on its position. If we make a curve of the occurrences along the chromosome, multiple peaks can be identified indicating the high frequencies of certain binding sites. We can set cut-off values for the core binding sites. Thus collect those sites with high occurrence numbers larger than cut off value as the core binding sites. From UCSC table browser (https://genome.ucsc.edu/cgi-bin/hgTables), we are able to get human RefSeq gene information. The locations of these core binding sites with human RefSeq files were compared with the midpoint of the fragments, such that the closest gene for each core

binding sites can be identified. These genes will be used for further functional annotation studies.

Distance Distribution of P53 Binding Sites

The chromatin context provides another perspective to see the regulation of p53-DNA binding. Many studies were revealed that p53 genomic binding patterns in normal cell lines is distinct from that in cancer cell lines, which means that the chromatin organizations around p53 binding sites are different between normal cells and cancer cells. It can help us understand the role of cell context, experimental conditions in p53 binding, mutation factors and influence of chromatin states on modulation of p53-DNA binding. Based on the collection of p53 binding sites mapped in normal cell lines and cancer lines, a statistic analyses on the distances to the transcription start sites (TSSs) of nearby genes was conducted. Different distribution situations were compared between these two sets of p53 binding sites. To test the hypothesis that there is significant difference between normal and cancer cell lines in chromatin distribution, we calculate the means and p-value of these two groups.

P53 Binding Sites Residing in Repeats

Many of the p53 binding sites (normal or cancer) are found locating in transposable repetitive regions in the human genome. Wei et al. [20] reported that over 30% of p53 sites are highly enriched in human ERV LTR regions. They collected only hundreds of p53 cancer binding sites. We collected much more p53 ChIP fragments including their dataset to get a more comprehensive result. Also it's important to compare the different repetitive distribution between normal and cancer cell lines. From the UCSC genome annotation database, we can get the human hg18 genome annotation files for each chromosome with the repeat regions. Then map the normal p53 BSs and cancer p53 BSs to the repeat regions based on their chromosome positions. We are able to get the number of repeat classes and repeat families in normal as well as cancer p53 BSs respectively and calculate the percentages of every

kind of repeats. Therefore we have a complete set of p53 binding sites residing in repetitive regions.

Functional Annotation of P53 ChIP Clusters

Large amount of p53 fragments are widely distributed in human genome and p53 tumor suppressor pathways have a high correlation with growth-inhibitory activity of 123 anticancer agents in more than 60 cell lines [21]. The single-nucleotide polymorphisms (SNPs) in the p53-pathway have apparent influence on the alteration of its function [22]. Several studies reported about the signaling pathways enriched in HCT116 [23] and IMR90 [24] by using the genes harboring p53 binding sites. They found the common pathway is p53 signaling pathway. But the most highly enriched pathways in HCT116 and IMR90 are different. Smeek et al. [25] also performed functional annotation for p53 phosphorylated at S46 and found that p53 signaling pathway is the most enriched cluster. The next two important functional categories are nuclear envelope and cell cycle regulation. So it is meaningful to analyze p53 pathways and function annotation.

DAVID (the Database for Annotation, Visualization and Integrated Discovery) is a bioinformatics resource used for functional interpretation of large lists of genes or proteins [26, 27]. So we can import the genes list of p53 ChIP clusters to DAVID to get their pathways. The DAVID Functional Annotation Clustering Tool also measures the relationships of annotation terms and show cluster groups [28]. We can compare the pathways and clusters differences between cancer and normal cell.

Results

Collection of P53 Binding Sites and Lengh-distribution

After searching and studying most published articles relating to p53 binding sites in vivo and in vitro, we have collected 154 p53 REs (Appendix Table A-1) and about 120,000 identified ChIP fragments from 25 datasets (Table 1). These ChIP segments are classified into 9 normal datasets and 16 cancer datasets according to cell type

under different treatments.

	Cell type	Cell line	Treatment	Exp. technique	Binding sites	Reference
Botcheva (2011)	normal	IMR90	5-FU	ChIP-seq	743	24
Zeron-Medina (2013)	normal	lympho blastoid	Nutlin 3a	ChIP-seq	1,084	29
			DXR		12,792	
			IR		152	
Akdemir (2014)	normal	hESC	DXR (Adr)	ChIP-seq	4,324	30
			RA (re)		7,197	
McDade (2014)	normal	keratin octye	DXR(Adr)	ChIP-seq	4,169	31
			cisplatin		8,629	
Su (2015)	normal	lympho blastoid	DXR	ChIP-seq	2,930	32
Wei (2006)	cancer	HCT11	5-FU	ChIP-PET	542	20
Smeenk (2008)	cancer	U2OS	Actinomycin D	ChIP-chip	1,545	33
Smeenk (2011)	cancer	U2OS	Etoposide	ChIP-seq	2,920	25
			Actinomycin D		2,132	
Nikulenkov (2012)	cancer	MCF7	Nutlin 3a	ChIP-seq	16,707	34
			RITA		10,622	
			5-FU		10,365	
Menendez	cancer	U2OS	Nutlin 3a	ChIP-seq	18,158	35

(2013)			DXR		3,087	
Botcheva (2014)	cancer	HCT116	5-FU	ChIP-seq	550	23
Rashi-Elkeles (2014)	cancer	CAL51	IR	ChIP-seq	1,825	36
Sanchez (2014)	cancer	HCT116	5-FU	ChIP-seq	3,668	37
Chang (2014)	cancer	U2OS	Nutlin 3a	ChIP-exo	952	38
			5-FU		1864	
			DXR		1303	
			UV		1556	

Table 1. Summary of p53 binding sites in vivo identified by ChIP experiments

After collecting all the p53 binding sites in Table 1, we separated them into normal cell lines and cancer cell lines separately. There are 77,796 p53 binding sites in cancer cell lines and 42,020 in normal cell lines.

Figure 4. Length - frequency distributions of ChIP segments.

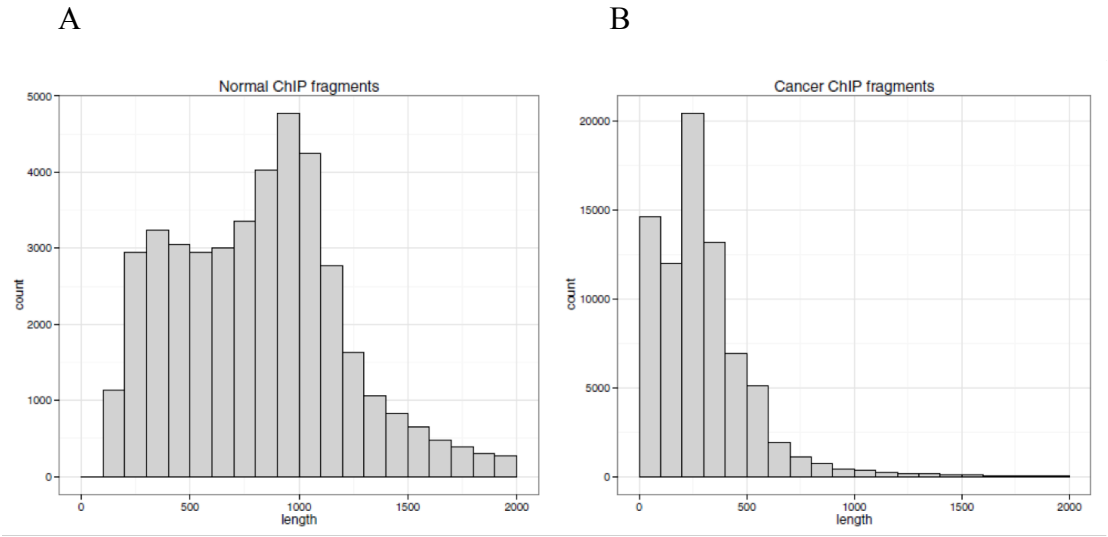

C

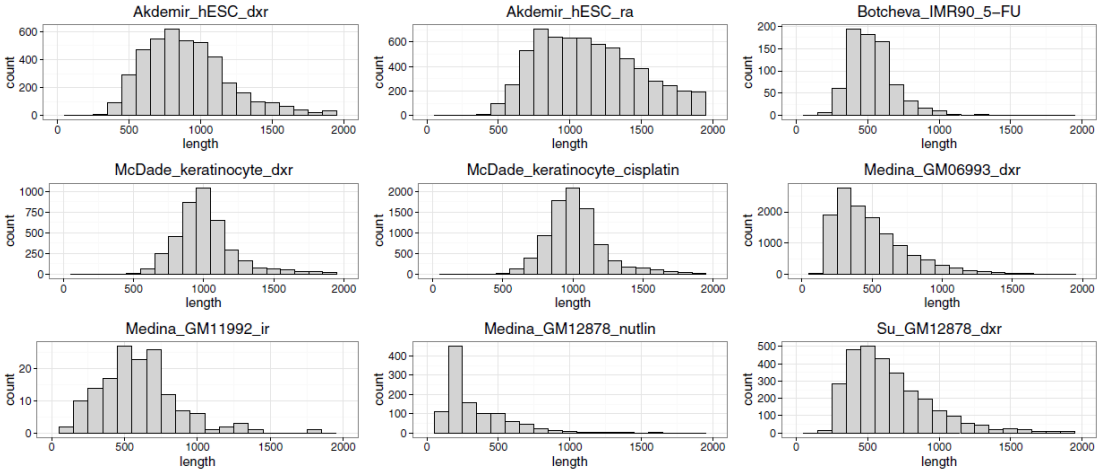

D

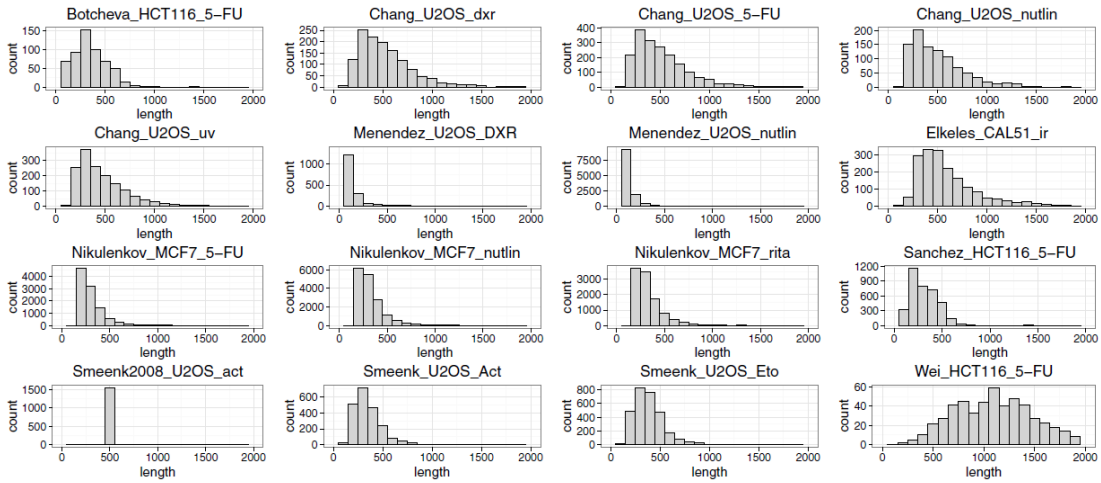

(A) Total 42020 normal segments length – frequency distribution. (B) Total 77796 cancer segments length – frequency distribution. (C) 9 normal datasets length – frequency distribution. (D) 16 cancer datasets length – frequency distribution.

Based on the start and end position of ChIP segments, the length distribution is firstly analyzed. The normal (Figure 4A) cell lines provide a wider length distribution than cancer (Figure 4B) cell lines. The lengths of p53 binding sites in cancer concentrate mainly on 0~500bp. While for normal cell lines, the lengths cover from 0~2000bp. It shows that cancer segments are much shorter than normal segments on average. The peak value of normal cell lines is around 1000pb while it is 500pb in

cancer cell lines. From every dataset length distribution, normal ChIP fragments are longer than cancer on average. We need to investigate the reasons for this difference in the future.

Concordance Between P53 Binding Sites Identified in Vitro and in Vivo

Based on work of Riley et al. [18], we collected 154 famous p53 REs (Appendix Table A-1). In the research of Riley et al. [14], they have 156 binding sites. We remove the human hepatitis B virus (HBV) site and one overlapping CDKN1A (p21) sites.

To study the correlation between p53 binding sites identified in vitro and in vivo, we imported all ChIP segments to UCSC Genome Browser to do visualization. Then mapped the targeted 154 REs based on their chromosomes and positions (Appendix Table A-1). All the custom track figures of p53 REs can be checked in Supplementary Figure S1.

We can find that 71 out of 154 (46%) REs overlap with ChIP fragments. So it is obvious that the ChIP segments can cover the most of targeted genes.

Figure 5. BBC3 (PUMA) gene in UCSC Genome Browser

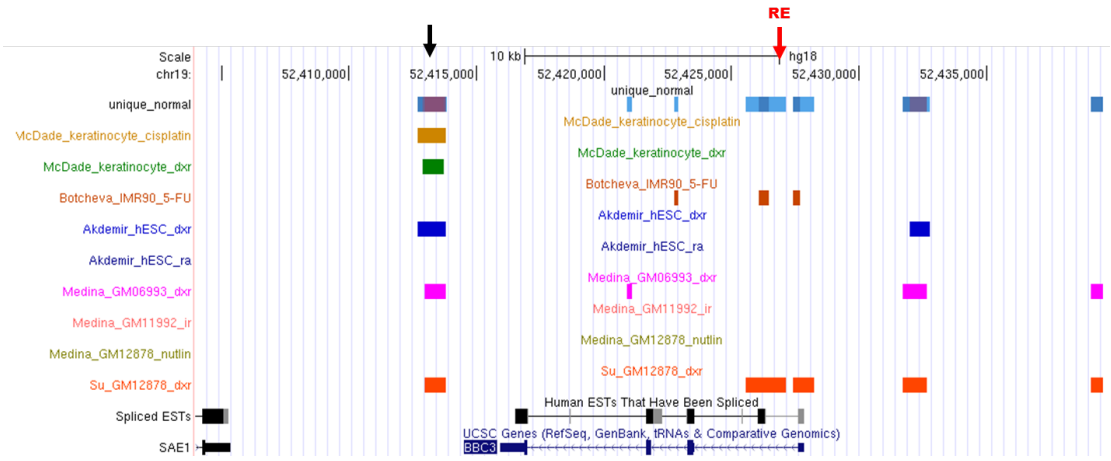

A (normal)

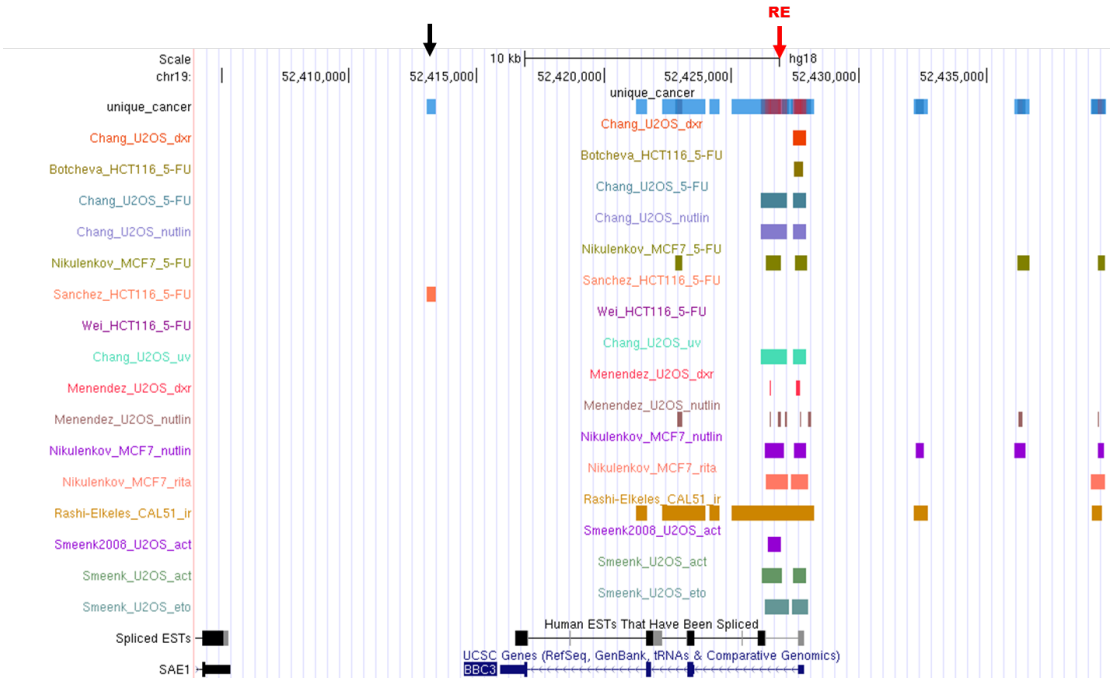

B (cancer)

Figure 5 shows one main famous target gene BBC3 (PUMA) overlaps with ChIP fragments locating in normal and cancer cell line separately through the UCSC Genome Browser. It concluded that the p53 binding sites identified in vitro has a very high concordance with those identified in vivo. Based on the figures, besides the targeted genes position, there are many other areas that are covered by many ChIP segments from different datasets. For example, the black arrows in Figure 5 point the common areas. It may help to better identify p53 binding sites relating these areas in the future.

Detection of P53 Core Binding Sites

Many p53 ChIP fragments have overlapping positions in the human genome (hg18), so we collected those sites with high occurrence numbers as the core set. After mapping all normal and cancer fragments to human genome (hg18) based on their chromosome positions, we found that 44% (18,565 out of 42,020) normal fragments are singletons and 40% (31,212 out of 77,796) cancer fragments are singletons. They do not overlap with other p53 binding sites. The other fragments

overlap with each other to be clusters. Based on there number of overlapping times, we denoted them as pile-2, pile-3, pile-4 and so on. For p53 normal fragments, the percentage of pile2 is 11% and pile 3 is 0.5%. P53 cancer cells have the similar percentage trend with normal cells. So we set the cut-off value of 3 to be core binding sites. That means that the fragments with occurrences equal or larger than 3 are core binding sites. We denoted them as "pile-3+". According to statistics, the normal pile-3+ containing 3551 fragments (Supplementary Table S1). While cancer pile-3+ has 6039 fragments (Supplementary Table S2).

Figure 6. Overlapping fragments between cancer clusters and normal clusters

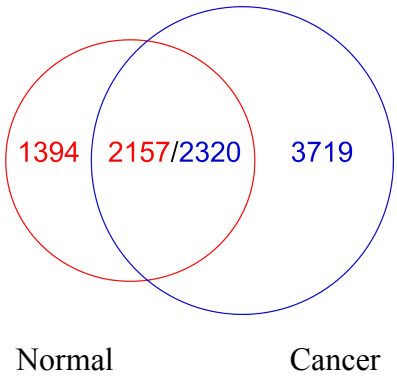

After comparing normal pile-3+ and cancer pile-3+, we found the Figure 7 overlapping results. Normal pile-3+ has 2157 fragments overlapping with cancer pile-3+ while cancer pile-3+ only has 2320. The reason is that the average normal fragments are longer than cancer fragments as we mentioned in previous length-frequency distribution analysis. So one fragment in normal cells may overlap more than one cancer fragment. For better description, we denote the p53 ChIP fragments that only belong to normal or cancer cells as "normal_only" group or "cancer_only" group. Also we name the overlapping fragments as "normal/cancer" group.

Distance Distribution of P53 Binding Sites

From UCSC Table Browser we downloaded human RefSeq Genes table with assembly hg18. Then mapped the normal and cancer pile-3+ fragments

(Supplementary Table S1, S2) to this table based on their positions to find nearest RefSeq genes. If the ChIP fragment is upstream to the transcription start site (TSS) of a give gene, the distance is '-'. Otherwise the distance has a '+' sign. The RefSeq gene names and distances are added to the pile-3+ table with column names "Gene Name" and "Peak to TSS" (Supplementary Table S1, S2).

Figure 7. Genomic distributions of pile-3+ binding sites (BSs) to TSSs

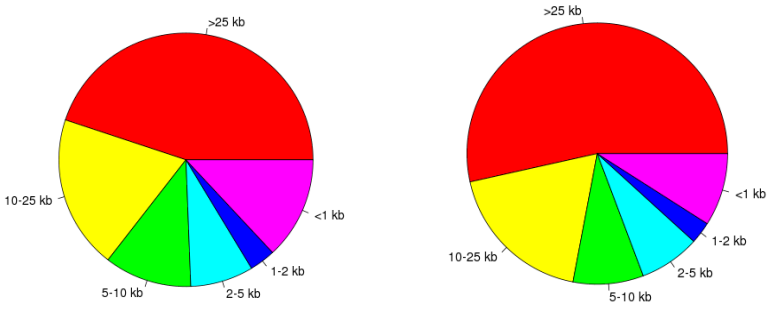

A. Normal B. Cancer

After a statistics analysis of the lengths from p53 binding sites to the transcriptional start sites (TSSs) in normal and cancer cell lines, it showed significant differences between the two cases in Figure 6. In cancer BSs the proportion of ">25kb" is much higher than normal. While the part "<1kb" is smaller in cancer than normal. On the whole, cancer p53 BSs are located far from TSSs and normal BSs are near the TSSs. This shows that they have the apparently different genomic distributions and chromatin context. We used the absolute distance values for hypothesis test and got the average distance 66389.03 for normal cell lines and 74972.97 for cancer cell lines. The p-value got from T-test is 0.00165, which is much smaller than 0.05. It demonstrates that there is significant difference in the distances between normal and cancer p53 clusters.

P53 Binding Sites Residing in Repeats

After mapping pile-3+ normal and cancer ChIP fragments (Supplementary Table S1, S2) to human genome annotation table based on their positions. We got repeated

name, repeated class and repeated family information for normal_only, cancer_only and normal/cancer groups and conducted a statistical analyses (Table 2). The repeated types include SINE (MIR, Alu), Simple Repeat, LTR, Low Complexity, LINE (CR1, L1, L2, RTE), DNA. The remaining repeated types with lower occurrences were added up to be "Other" category.

If the ChIP fragments are not in any repeat areas, they are classified as "Not_in_repeat" category. If the ChIP fragments cover more than one repeat area, all the repeat categories are counted.

A:

	Normal		Normal/Cancer		Cancer	
All repeat types	Count	Percentage	Count	Percentage	Count	Percentage
SINE	1382	39.09%	1260	28.42%	1568	26.79%
Simple_repeat	342	9.67%	334	7.53%	323	5.52%
Other	45	1.27%	21	0.47%	69	1.18%
Not_in_repeat	166	4.70%	479	10.81%	1268	21.66%
LTR	455	12.87%	1046	23.60%	843	14.40%
Low_complexity	332	9.39%	213	4.80%	259	4.43%
LINE	618	17.48%	827	18.66%	1139	19.46%
DNA	195	5.52%	253	5.71%	384	6.56%
Total	3535	100.00%	4433	100.00%	5853	100.00%

B:

	Normal		Normal/Cancer		Cancer	
SINE	Count	Percentage	Count	Percentage	Count	Percentage
MIR	526	38.06%	461	36.59%	570	36.35%
Alu	856	61.94%	799	63.41%	998	63.65%
Total	25	4.05%	1260	100.00%	50	4.39%

C:

	Normal		Normal/Cancer		Cancer	
LINE	Count	Percentage	Count	Percentage	Count	Percentage
CR1	25	4.05%	41	4.96%	50	4.39%
L1	305	49.35%	488	59.01%	616	54.08%
L2	280	45.31%	285	34.46%	462	40.56%
RTE	8	1.29%	13	1.57%	11	0.97%
Total	618	100.00%	827	100.00%	1139	100.00%

D:

	Normal		Normal/Cancer		Cancer	
Alu	Count	Percentage	Count	Percentage	Count	Percentage
AluJb	111	12.97%	133	16.65%	153	15.33%
AluJo	125	14.60%	147	18.40%	150	15.03%
AluSc	25	2.92%	27	3.38%	32	3.21%
AluSg	64	7.48%	40	5.01%	69	6.91%
AluSg/x	14	1.64%	23	2.88%	32	3.21%
AluSp	45	5.26%	30	3.75%	35	3.51%
AluSq	68	7.94%	51	6.38%	70	7.01%
AluSx	247	28.86%	227	28.41%	256	25.65%
AluY	79	9.23%	42	5.26%	88	8.82%
FLAM_A	12	1.40%	8	1.00%	19	1.90%
FLAM_C	20	2.34%	24	3.00%	31	3.11%
FRAM	15	1.75%	18	2.25%	30	3.01%
Other	31	3.62%	29	3.63%	33	3.31%
Total	856	100.00%	799	100.00%	998	100.00%

Table 2: The statistics results of p53 ChIP fragments in repetitive regions. Statistics are shown for (A) All repeat types; (B) Short interspersed nuclear elements (SINE); (C) Long interspersed nuclear elements (LINE); (D) Alu elements.

Here we focused on their distributions in all repeat types, short interspersed nuclear elements (SINE), long interspersed nuclear elements (LINE) and Alu elements. Based on percentages of various repeat categories, the pie charts are shown for better display (Figure 8).

Figure 8. Pie charts of p53 clusters residing in repeat regions

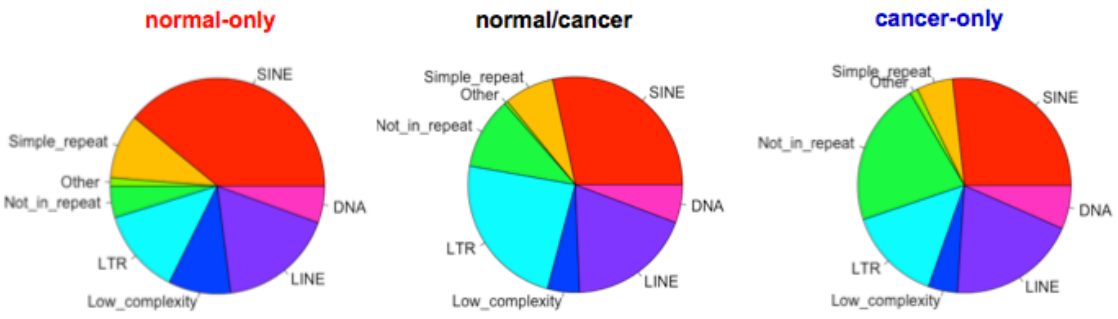

A B C

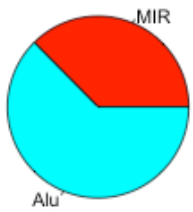

D

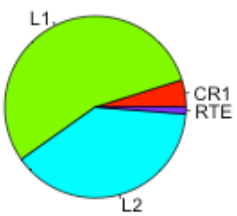

E

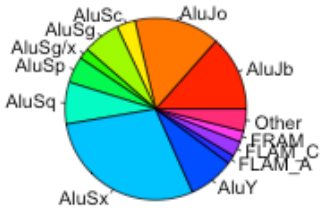

F

G

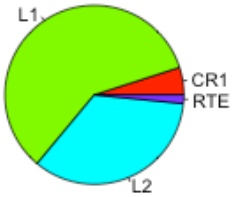

H

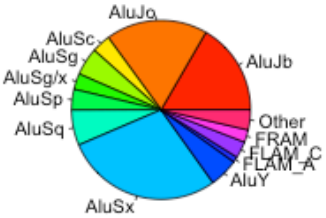

I

J

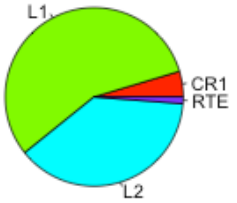

K

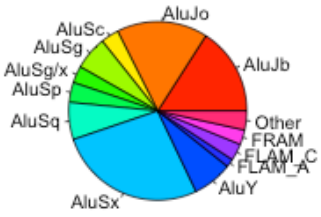

L

(A) All repeat types for normal_only group. (B) All repeat types for normal/cancer group. (C) All repeat types for cancer_only group. (D) Short interspersed nuclear elements (SINE) for normal_only group. (E) Long interspersed nuclear elements (LINE) for normal_only group. (F) Alu elements for normal_only group. (G) Short interspersed nuclear elements (SINE) for normal/cancer group. (H) Long interspersed nuclear elements (LINE) for normal/cancer group. (I) Alu elements for normal/cancer group. (J) Short interspersed nuclear elements (SINE) for cancer_only group. (K) Long interspersed nuclear elements (LINE) for cancer_only group. (L) Alu elements for cancer_only group.

Based on the statistic results (Table 2) and pie charts (Figure 8), we can find that

normal cells have a big difference in the distribution of repetitive regions compared with cancer cells. For p53 binding sites in normal_only group, highest proportion "SINE" category reaches 39%. While in normal/cancer and cancer_only group, "SINE" only has 26% and 28%. The biggest difference is the sites that are not in any repetitive regions. In normal_only group, "Not_in_repeat" is only 4.7%. But in cancer_only group there are 10% of ChIP fragments that are not in any repetitive regions. The percentage of "LTR" in normal/cancer group is much higher than normal_only and cancer_only groups. It reaches 23%, which demonstrates the conclusion that one-third of p53 binding sites containing LTRs [14].

In the repeated family "SINE" (Figure 8D, Figure 8G, Figure 8J), "LINE" (Figure 8E, Figure 8H, Figure 8K) and "Alu" elements (Figure 8F, Figure 8I, Figure 8L), there are no evidential differences among cancer_only, normal/cancer and normal_only groups. In the "SINE" repeat family, "Alu" can reach to about 60% in all of them.

Functional Annotation of P53 ChIP Clusters

In Figure 6, most of the p53 ChIP clusters are located far away from TSSs (>10 kb). Thus the genes of p53 binding sites with the distances 5kb upstream/downstream of transcription start sites (TSSs) were selected as our targeted genes. We have got the genes list of p53 ChIP fragments in previous "Distance Distribution" step. So we imported gene lists of normal_only, normal/cancer and cancer_only groups to DAVID (https://david.ncifcrf.gov/). From DAVID Pathway Viewer, obviously we can find Kyoto Encyclopedia of Genes and Genomes (KEGG) database containing genes from list. The following Figure 9 shows the significant KEGG pathways of normal_only, normal/cancer and cancer_only groups. We chose the pathways with statistical significant p-value < 0.01.

Figure 9. Enriched pathways for p53 genes from DAVID

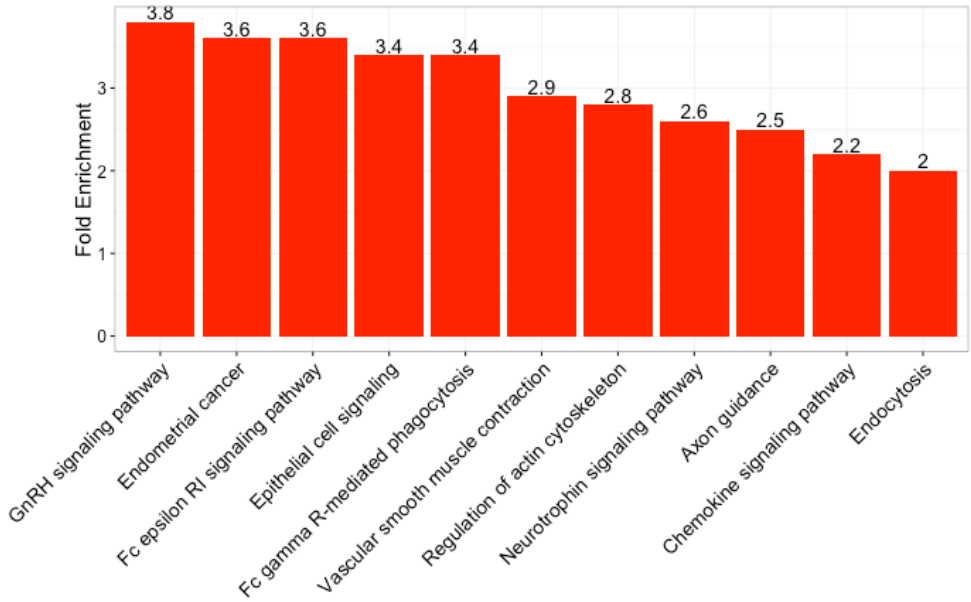

A

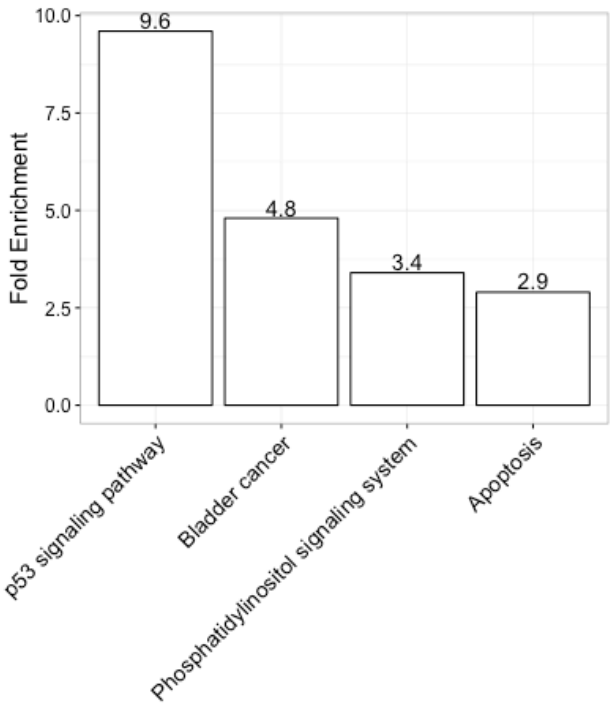

B

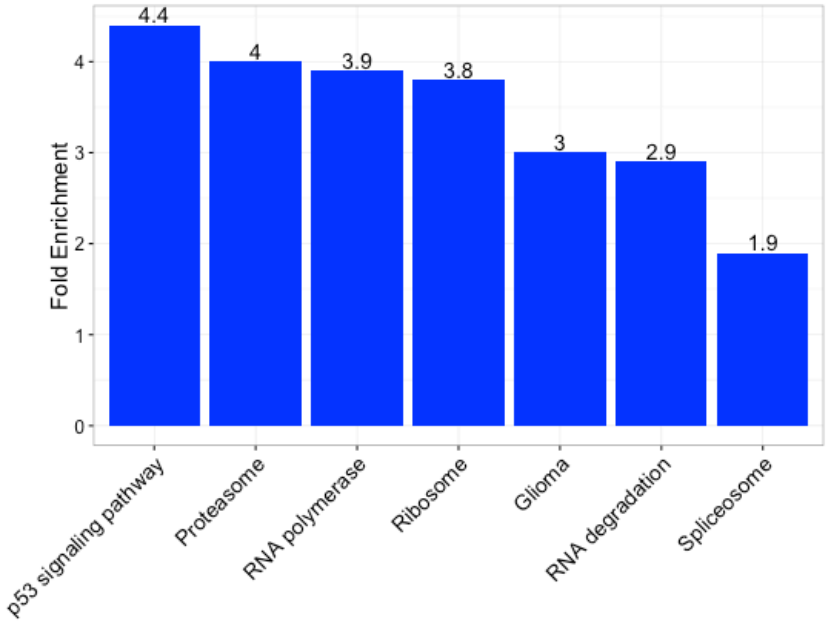

C

Most highly enriched KEGG pathway in DAVID functional annotation analysis of the genes associated with p53 ChIP fragments (p-value <0.01). Fold enrichment is calculated by DAVID. (A) Normal_only group. (B) Normal/cancer group. (C) Cancer_only group.

Figure 9A, 9B, 9C show the enriched KEGG pathways for normal_only, normal/cancer and cancer_only groups. P53 signaling pathway in both normal/cancer and cancer_only group has the highest fold enrichment values 9.6 and 4.4. In normal/cancer group, three other groups are also showed, “bladder cancer”, “apoptosis” and “phosphatidylinositol signaling system”. The changes in the molecules in the p53 genes and pathways can regulate the cell cycle and affect bladder cancer [39]. Haupt et al. [40] reported that p53 activates signals through two major apoptotic pathways: the extrinsic, death receptor pathway and the intrinsic, mitochondrial pathway. The tumor suppressor PTEN antagonizing phosphatidylinositol-3,4,5-trisphosphate (PIP3) regulates p53 pathway [41]. These prove that the pathways from our p53 ChIP fragments are involved in the p53

transcriptional programs.

Figure 10. Enriched clusters for p53 genes from DAVID

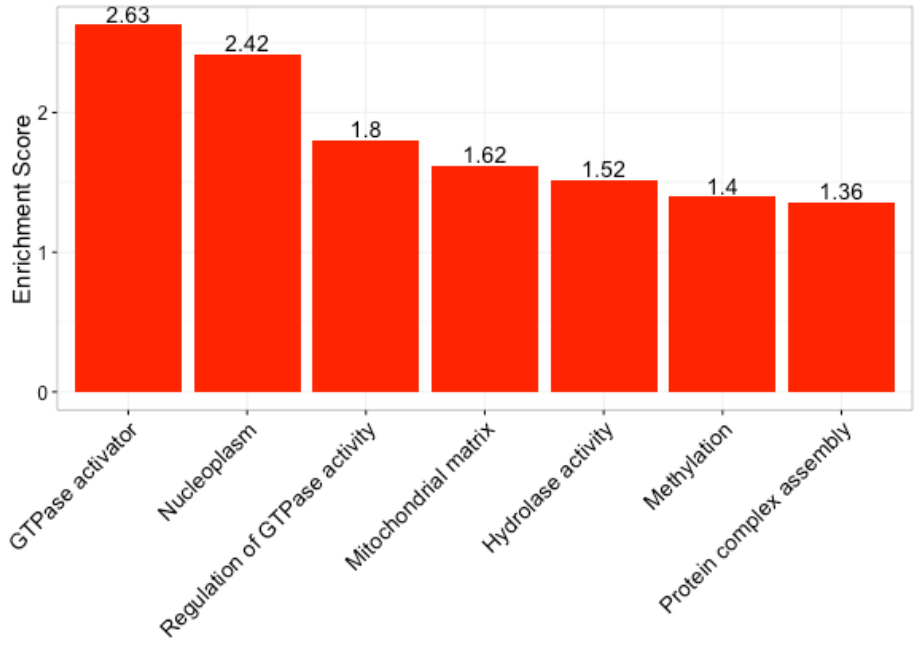

A

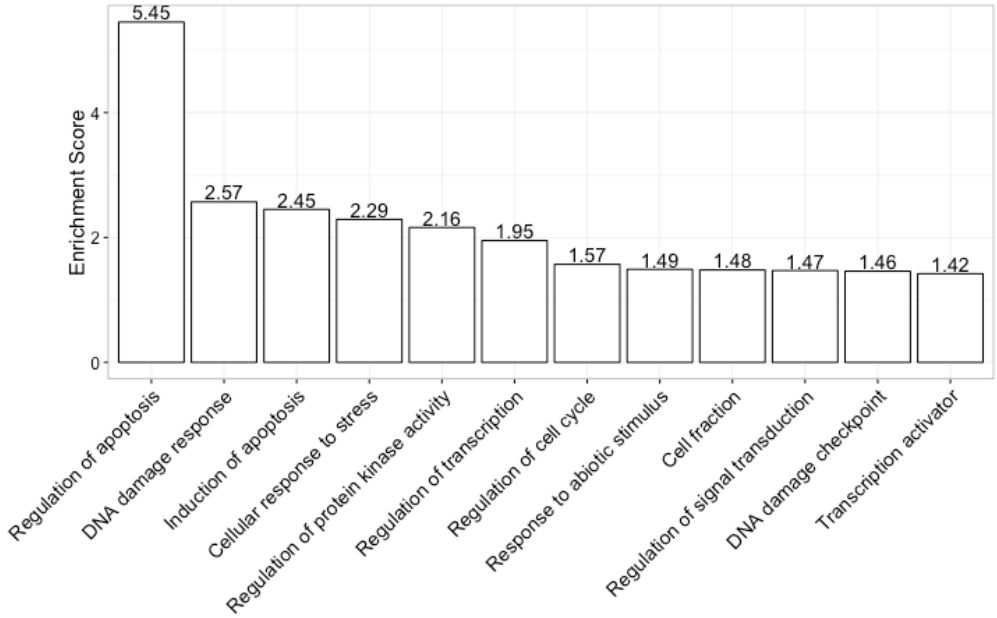

B

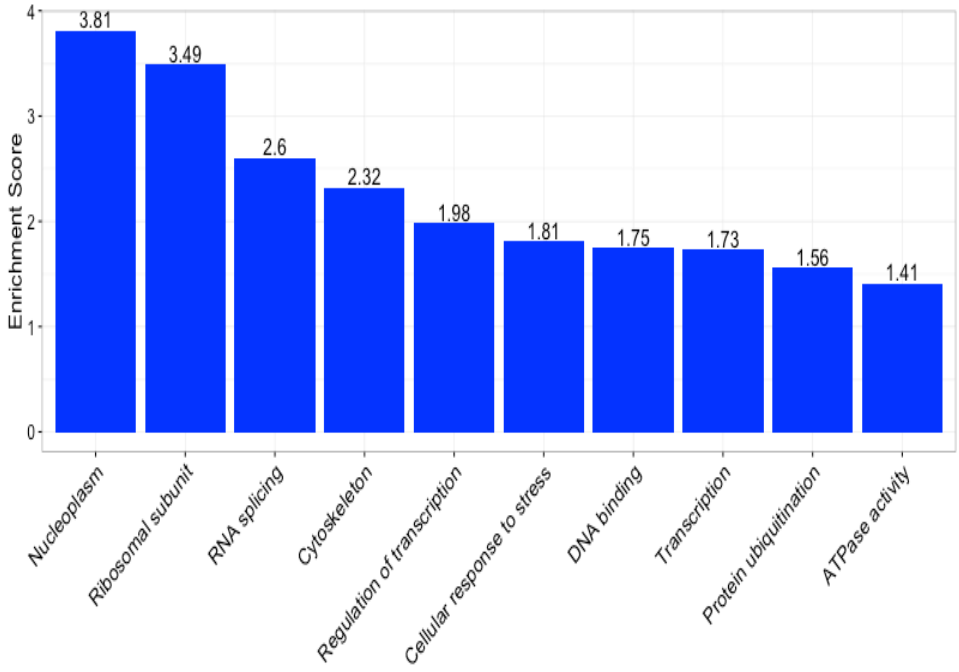

C

Figure 10: Most highly enriched clusters in DAVID functional annotation analysis of the genes associated with p53 ChIP fragment. See Supplementary Table S8-S9 for all enriched clusters. (A) Normal_only group. (B) Normal/cancer group. (C) Cancer_only group.

Figure 10A, 10B, 10C show the highly enriched clusters of genes for normal_only, normal/cancer and cancer-only groups. They are arranged based on the enrichment scores. From normal/cancer groups (Figure 10B), we can find that the most significant GO terms include ‘‘Regulation of apoptosis’’, “DNA damage response” and “Cellular response to stress”. These demonstrate that the p53 clusters from p53 ChIP fragments are bound up with genes relating with cell cycle control and apoptosis.

Discussion

Chromatin Context and Distribution

P53 plays an important role in regulating cell cycles and maintaining genomic stability. The transcription regulation can be influenced by many factors. Leroy et al. [42] reported that more than half of human cancers carry TP53 gene mutations and these relate with p53 REs. Posttranslational Modification can impact the p53 function in response to genotoxic or nongenotoxic stresses [43]. Some family members like p63 and p73 can also influence p53 activities [44]. All these factors active in the p53 chromatin context because p53 plays a role in transcription regulation and interactions with DNA. In this study, different p53 chromosome distributions and organizations between normal and cancer cell lines were analyzed using ~120,000 ChIP fragments.

As our datasets are comprehensive and cover most published p53 DNA binding sites in vivo, the normal and cancer cell lines are under the same treatments (Table 1). For example, both of them have treatments like 5-FU, Nutlin 3a, DXR. Actually these datasets come from different experiments, labs and researches. From our results in "Concordance between P53 Binding Sites and ChIP Fragments" and "Core Binding Sites", there were consistently large overlapping areas. So the chromatin context analyses in our research has statistic significance.

P53 Distributions in Repetitive Regions in Normal and Cancer Chromatin

The majority of p53 binding sites locate in many repetitive regions: SINE, LINE, Alu and so on. Cui et al. [45] proposed that the primate-specific Alu repeats involve in changing the p53 regulatory network in the chromatin context. In this study, we focus on the different repetitive distributions between normal and cancer cell lines relating with chromatin context. For example, cancer_only group has a much larger "Not_in_repeat" percentage than normal_only group. This may result from their different chromatin organization. Many factors probably influence this different distribution, like the p53 binding activity, DNA hypomethylation in cancer cells.

Future Work

This study is focused on p53 binding sites configuration. The differences of chromatin context and distribution between cancer cell lines and normal cell lines have been analyzed from several aspects, such as length distributions of p53 binding sites, overlapping areas, distribution of various repeat categories and enriched pathways and clusters. Additional research and work can be investigated based on this p53 dataset.

From the visualization results of these ~120,000 ChIP fragments, we can find that it covers about 46% of the 154 REs list. There still have 54% percentages of REs are not included. Also from Table 1, the normal and cancer cell lines were found to share many several treatments. But some treatments just belong to one cell type. For example, normal ChIP fragments have cisplain treatment while cancer does not have. These mean our dataset still needs supplement in the future, which can provide more instructive results.

Millau et al. [46] reported that the chromatin is the reason for the formation of stress-specific p53 binding patterns. The sequence-specific p53 binding affinity cannot change the p53 binding patterns. While some treatments, like UVB, Nutlin-3, can get different cellular results. In our research, we collected large number of p53 ChIP fragments to form a distinct p53 binding patterns consisting of normal and cancer cell lines. Further analysis can be carried out on our p53 binding patterns with stress treatments. We can see how p53 has specific gene regulation in response to stress in normal and cancer cell lines.

Conclusions

This thesis research involved many public ChIP data to do p53 chromatin context study. All the largest amount of data were analyzed by computer language R and performed on the public bioinformatics platform, like UCSC, DAVID. The comparison of chromatin organization and distribution between normal cell lines and cancer cell lines can help us have more pertinent and specific research in the future. From our statistic results, we tested the hypothesis and demonstrate that normal can

cancer cell lines have different chromatin distribution. We also reveal the enriched pathways and clusters to demonstrate p53 transcriptional function, which represents the direction and emphasis for future analysis.

References

1. Hyland, E.M., Cosgrove, M.S., Molina, H., Wang, D., Pandey, A., Cottee, R.J. and Boeke, J.D. (2005). Insights into the Role of Histone H3 and Histone H4 Core Modifiable Residues in Saccharomyces cerevisiae. Mol Cell Biol. 25, 10060-10070.
2. Cole, H.A., Cui, F., Ocampo, J., Burke, T.L., Nikitina, T., Kotomura, N., Zhurkin, V.B. and Clark, D.J. (2016) Novel nucleosomal particles containing core histones and linker DNA but no histone H1. Nucleic Acids Res. 44, 573-581.
3. Henikoff, S., Furuyama, T. and Ahmad, K. (2004). Histone variants, nucleosome assembly and epigenetic inheritance. Trends in Genetics. 20, 320-326.
4. Bartke, T., et al. (2010). Nucleosome-interacting proteins regulated by DNA and histone methylation. Cell 143(3): 470-484.
5. Bernstein, B.E., Meissner, A., Lander, E.S. The mammalian epigenome. Cell. 2007; 128, 669–681.
6. Rossetti, L., Cacchione, S., De Menna, A., Chapman, L., Rhodes, D. and Savino, M. (2001) Specific interactions of the telomeric protein Rap1p with nucleosomal binding sites. J. Mol. Biol. 306, 903-913.
7. Sengupta, S.M., VanKanegan, M., Persinger, J., Logie, C., Cairns, B.R., Peterson, C.L. and Bartholomew, B. (2001) The interactions of yeast SWI/SNF and RSC with the nucleosome before and after chromatin remodeling. J. Biol. Chem. 276, 12636-12644.
8. Harris, C. C. (1996). Structure and function of the p53 tumor suppressor gene: clues for rational cancer therapeutic strategies. Journal of the National Cancer Institute 88(20): 1442-1455.
9. Hollstein, M., K. Rice, M. S. Greenblatt, T. Soussi, R. Fuchs, T. Sorlie, E. Hovig, B. Smith-Sorensen, R. Montesano, and C. C. Harris. 1994. Database of p53 gene somatic mutations in human tumors and cell lines. Nucleic Acids Res. 22:3551–3555.

10. Appella, E. and Anderson, C.W. (2001) Post-translational modifications and activation of p53 by genotoxic stresses. Eur. J. Biochem. 268, 2764-2772.
11. Kaeser, M. D. and Iggo, R. D. (2002). Chromatin immunoprecipitation analysis fails to support the latency model for regulation of p53 DNA binding activity in vivo. Proc Natl Acad Sci U S A 99(1): 95-100.
12. Nagaich, A.K., Zhurkin, V.B., Durell, S.R., Jernigan, R.L., Appella, E. and Harrington, R.E. (1999) p53-induced DNA bending and twisting: p53 tetramer binds on the outer side of a DNA loop and increases DNA twisting. Proc Natl Acad Sci USA 96, 1875-1880.
13. Sahu, G., Wang, D., Chen, C.B., Zhurkin, V.B., Harrington, R.E., Appella, E., Hager, G.L. and Nagaich, A.K. (2010) p53 binding to nucleosomal DNA depends on the rotational positioning of DNA response element. J. Biol. Chem. 285, 1321-1332.
14. Wang, T., Zeng, J., Lowe, C.B., Sellers, R.G., Salama, S.R., Yang, M., Burgess, S.M., Brachmann, R.K., Haussler, D. (2007) Species-specific endogenous retroviruses shape the transcriptional network of the human tumor suppressor protein p53. Proc. Natl. Acad. Sci. U.S.A. 104, 18613-18618.
15. Zemojtel, T., Kielbasa, S.M., Arndt, P.F., Chung, H-R. and Vingron, M. (2009) Methylation and deamination of CpGs generate p53-binding sites on a genomic scale. Trends Genet. 25, 63-66.
16. Harris, C.R., Dewan, A., Zupnick, A., Normart, R., Gabriel, A., Prives, C., Levine, A.J. and Hoh, J. (2009) p53 response elements in human retrotransposons. Oncogene 28, 3857-3865.
17. Leonova, K.I., Brodsky, L.B., Lipchick, B., Pal, M., Novototskaya, L., Chenchik, A.A., Sen, G.C., Komarova, E.A. and Gudkov, A.V. (2012) p53 cooperates with DNA methylation and a suicidal interferon response to maintain epigenetic silencing of repeats and noncoding RNAs. Proc. Natl. Acad. Sci. U.S.A. 110, E89-E98.
18. Riley, T., Sontag, E., Chen, P. and Levine, A. (2008) Transcriptional control of human p53-regulated genes. Nat. Rev. Mol. Cell Biol. 9, 402-412.

19. Cawley, S., Bekiranov, S., Ng, H.H., Kapranov, P., Sekinger, E.A., Kampa, D., Piccolboni, A.,Sementchenko, V., Cheng, J., Williams, A.J., Wheeler, R., Wong, B., Drenkow, J., Yamanaka, M., Patel, S., Brubaker, S., Tammana, H., Helt, G., Struhl, K., Gingeras, T.R (2004) Unbiased mapping of transcription factor binding sites along human chromosome 21 and 22 points to widespread regulation of noncoding RNAs. Cell 116, 499-509.

20. Wei, C. L., Wu, Q., Vega, V. B., Chiu, K. P., Ng, P., Zhang, T., Ruan, Y. (2006). A global map of p53 transcription-factor binding sites in the human genome. Cell, 124(1), 207-219.

21. O'Connor, J. J., Jackmamn, J.J., Timothy, I.B., Myers, G., Fan, S., Mutoh, M,. et al. (1997). Characterization of the p53 Tumor Suppressor Pathway in Cell Lines of the National Cancer Institute Anticancer Drug Screen and Correlations with the Growth-Inhibitory Potency of 123 Anticancer Agents. Cancer Research, 57, 4285-4300.

22. Sucheston, L., Witonsky, D.B., Hastings, D., Yildiz, O., Clark, V.J., Rienzo, A.D., and Onel, K. (2011). Natural selection and functional genetic variation in the p53 pathway. Human Molecular Genetics, 20, 1502-1508.

23. Botcheva, K., & McCorkle, S. R. (2014). Cell context dependent p53 genome-wide binding patterns and enrichment at repeats. PLoS One, 9(11), e113492.

24. Botcheva,K., McCorkle,S.R., McCombie,W.R., Dunn,J.J. and Anderson,C.W. (2011) Distinct p53 genomic binding patterns in normal and cancer-derived human cells. Cell Cycle 10, 4237-4249.

25. Smeenk, L., van Heeringen, S. J., Koeppel, M., Gilbert, B., Janssen-Megens, E., Stunnenberg, H. G., & Lohrum, M. (2011). Role of p53 serine 46 in p53 target gene regulation. PLoS One, 6(3), e17574.

26.Huang, D.W., Sherman, B.T. and Lempicki, R.A. (2009) Systematic and integrative analysis of large gene lists using DAVID Bioinformatics Resources. Nature Protoc., 4, 44-57.

27 Huang, D.W., Sherman, B.T. and Lempicki, R.A. (2009) Bioinformatics

enrichment tools: paths toward the comprehensive functional analysis of large gene lists. Nucleic Acids Res., 37, 1-13.

28. Huang, D.W., Sherman, B.T., Tan, Q., Kir, J., Liu, D. et al (2007) DAVID Bioinformatics Resources: expanded annotation database and novel algorithms to better extract biology from large gene lists. Nucleic Acid Research. 35, 169-175.
29. Zeron-Medina, J., Wang, X., Repapi, E., Campbell, M. R., Su, D., Castro-Giner, F., Bond, G. L. (2013). A polymorphic p53 response element in KIT ligand influences cancer risk and has undergone natural selection. Cell, 155(2), 410-422.
30. Akdemir, K. C., Jain, A. K., Allton, K., Aronow, B., Xu, X., Cooney, A. J., Barton, M. C. (2014). Genome-wide profiling reveals stimulus-specific functions of p53 during differentiation and DNA damage of human embryonic stem cells. Nucleic Acids Res, 42(1), 205-223.
31. McDade, S. S., Patel, D., Moran, M., Campbell, J., Fenwick, K., Kozarewa, I., McCance, D. J. (2014). Genome-wide characterization reveals complex interplay between TP53 and TP63 in response to genotoxic stress. Nucleic Acids Res, 42(10), 6270-6285.
32. Su, D., Wang, X., Campbell, M. R., Song, L., Safi, A., Crawford, G. E., & Bell, D. A. (2015). Interactions of chromatin context, binding site sequence content, and sequence evolution in stress-induced p53 occupancy and transactivation. PLoS Genet. 11(1): e1004885.
33. Smeenk, L., van Heeringen, S. J., Koeppel, M., van Driel, M. A., Bartels, S. J., Akkers, R. C., Lohrum, M. (2008). Characterization of genome-wide p53-binding sites upon stress response. Nucleic Acids Res, 36(11), 3639-3654.
34. Nikulenkov, F., Spinnler, C., Li, H., Tonelli, C., Shi, Y., Turunen, M., Selivanova, G. (2012). Insights into p53 transcriptional function via genome-wide chromatin occupancy and gene expression analysis. Cell Death Differ, 19(12), 1992-2002.
35. Menendez, D., Nguyen, T. A., Freudenberg, J. M., Mathew, V. J., Anderson, C. W., Jothi, R., & Resnick, M. A. (2013). Diverse stresses dramatically alter genome-wide p53 binding and transactivation landscape in human cancer cells. Nucleic Acids Res, 41(15), 7286-7301.

36. Rashi-Elkeles, S., Warnatz, H. J., Elkon, R., Kupershtein, A., Chobod, Y., Paz, A., Shiloh, Y. (2014). Parallel profiling of the transcriptome, cistrome, and epigenome in the cellular response to ionizing radiation. Sci Signal, 7(325), rs3.

37. Sanchez, Y., Segura, V., Marin-Bejar, O., Athie, A., Marchese, F. P., Gonzalez, J., Huarte, M. (2014). Genome-wide analysis of the human p53 transcriptional network unveils a lncRNA tumour suppressor signature. Nat Commun, 5, 1-13.

38. Chang, G. S., Chen, X. A., Park, B., Rhee, H. S., Li, P., Han, K. H., Pugh, B. F. (2014). A comprehensive and high-resolution genome-wide response of p53 to stress. Cell Rep, 8(2), 514-527.

39. Mitra, A.P., Birkhahn, M., Cote, R.J. (2007) p53 and retinoblastoma pathways in bladder cancer. World Journal of Urology. 25, 563-571.

40. Haupt, S., Berger, M., Goldberg, Z., Haupt, Y. (2003). Apoptosis – the p53 network. Journal of Cell Science. 115, 4077-4085.

41. Bunney, T.D. and Katan, M. (2010) Phosphoinositide signaling in cancer: beyond PI3K and PTEN. Nat. Rev. Cancer, 10, 342-352.

42. Leroy, B., Anderson, M. and Soussi, T. (2014). TP53 mutations in human cancer: database reassessment and prospects for the next decade. Hum. Mutat. 35, 672–688.

43. Meek, D. W. and Anderson, C. W. (2009). Posttranslational modification of p53: cooperative integrators of function. Cold Spring Harb. Perspect. Biol. 1:a000950.

44. Botcheva, K. (2014). p53 binding to human genome: crowd control navigation in chromatin context. Frontiers in Genetics. 22, 447-453.

45 Cui, F., Sirotin, M.V. and Zhurkin, V.B. (2011) Impact of Alu repeats on the evolution of human p53 binding sites. Biol. Direct, 6, 2.

46. Millau, J.F., Bandele, O.J., Perron, J., Bastien, N., Bouchard, E.F., Gaudreau, L., Bell, D.A. and Drouin, R. (2010) Formation of stress-specific p53 binding patterns is influenced by chromatin but not by modulation of p53 binding affinity to response elements. Nucleic Acids Res., 39, 3053-3063.

Appendix A

Name	Chr	Strand	Start	End	1st half-site	Spacer	2nd half-site	Overlap with ChIP?
ABCB1	7	—	87068176	87068208	GGGCAGGAAC	agcgccggggcgt	GGGCTGAGCA	No
ACTA2	10	—	90702802	90702821	AACCATGCCT		GCATCTGCCC	No
AIFM2_RE1	10	—	71563263	71563292	AGGCATGAGC	caccgtgcct	GGCCATGCCC	No
AIFM2_RE2	10	—	71563350	71563377	GGTCTCGCTA	tgttgccc	AGGCTGGTCT	No
ANLN	7	+	36395090	36395115	GAACTGGCTT	ttctga	GGGCCAGGCC	No
APAF1	12	+	97562605	97562637	AGACATGTCT	ggagaccctagga	CGACAAGCCC	Yes
APC	5	+	112101252	112101283	GGGCATACCC	ccgaggggtacg	GGGCTAGGGC	No
ARID3A	19	+	884568	884587	GGACACGCTG		GGACATGCCT	Yes
ATF3	1	+	210848347	210848383	AGTCATGCCG	ctggcttgggcaccatt	GGTCATGCCT	Yes
BAI1	8	+	143559821	143559840	GTGGCTGCCT		GGACATGTTC	Yes
BAX	19	+	54150282	54150301	GGGCAGGCCC		GGGCTTGTCG	Yes
BBC3	19	—	52426417	52426436	CTGCAAGTCC		TGACTTGTCC	Yes
BCL2L14	12	+	12117280	12117299	AGCCAAGGCT		GGTCTTGAAC	No
BCL6	3	—	188945441	188945472	GACAGTGCTT	gggggtgattc	GGGCTAGTCT	No
BDKRB2	14	+	95740864	95740883	GGAagTGCCC		AGGaggcTga	Yes
BID	22	—	16619483	16619502	GGGCATGATG		GTGCATGCCT	No
BIRC5	17	+	73721905	73721927	GGGCGTGCGC	tcc	CGACATGCCC	No
BNIP3L	8	+	26331013	26331037	AAGCTAGTCT	cagtg	GcGCATGCCT	No
BTG2	1	+	201541261	201541280	AGTCCGGGCA		GAGCCCGAGC	Yes
C12orf5	12	+	4301042	4301063	AGACATGTCC	ac	AGACTTGTCT	Yes
C13orf15	13	+	40930827	40930849	AGGCgAGTTT	aag	cAGCTTGTCC	No
CASP1	11	—	104411147	104411166	AGACATGCAT		ATGCATGCAc	No
CASP10	2	+	201755017	201755041	AAACTTGCTg	gttta	AAtCTTGgCT	No
CASP6	4	—	110838081	110838104	AGGCAAGGAG	tttg	AGACAAGTCT	No
CAV1	7	+	115952057	115952087	GCCCAAGCAC	cccagcgcggg	AGAaACGTTC	Yes
CCNG1	5	+	162797510	162797529	GcACAAGCCC		AGGCTAGTCC	Yes
CCNK	14	+	99020378	99020399	AAACTAGCTT	gc	AGACATGCTg	Yes
CD82	11	+	44542897	44542921	AGGCAAGCTG	gggca	GctCAAGCCT	Yes
CDC25C	5	—	137695540	137695570	GGGCAAGTCT	taccatttcca	GAGCAAGCaC	No
CDKN1A_RE1	6	+	36752204	36752223	GAACATGTCC		cAACATGTTg	Yes
CDKN1A_RE2	6	+	36753091	36753110	AGACTGGGCA		TGTCTGGGCA	Yes
CHMP4C	8	+	82806745	82806782	AAACAAGCCC	agtagcagcagctgctcc	GAGCTTGCCC	No
COL18A1_RE1	21	+	45697015	45697034	TGACATGTGT		GAGCATGTAT	No
COL18A1_RE2	21	+	45697491	45697510	TGACATGTGT		GAGCATGTAT	No
CRYZ	1	—	74963572	74963594	ctGCAAGTCC	att	AAACcTGTTT	No
CTSD_RE1	11	—	1741923	1741942	AAGCTgGgCC		GGGCTgaCCC	No

CTSD_RE2	11	—	1742152	1742171	AAcCTTGgTT		tgcAAgAgGC	No
CX3CL1	16	+	55963635	55963655	GGGCATGTTC	c	CAGCTTGTGG	No
DDB2	11	+	47193106	47193126	GAACAAGCCC	t	GGGCATGTTT	Yes
DDIT4	10	+	73703380	73703399	AAACAAGTCT		TTCCTTGATC	Yes
DDR1	6	+	30962949	30962968	GAGCTGGTCC		AGGCTTATCT	No
DKK1	10	+	53741910	53741935	AGCCAAGCTT	ttaatg	AACCAAGTTC	No
DNMT1	19	—	10166756	10166782	GCGCATGCGT	gttccct	GGGCATGGCC	No
DUSP1	5	—	172129554	172129574	GGTCCTGCCC	a	GGCAAATGGG	No
DUSP5	10	+	112246487	112246507	CAACAAGCCC	t	TGTCTAGTGC	No
EDN2	1	—	41720668	41720687	CTGCAAGCCC		GGGCATGCCC	Yes
EEF1A1_RE1	6	—	74285585	74285606	GGGCAGaCCC	ga	GAGCATGCCC	No
EEF1A1_RE2	6	—	74285784	74285805	AAACATGaTT	ac	AGGgACaTCT	No
EEF1A1_RE3	6	—	74286408	74286431	GGACACGTag	attc	GGGCAAGTCC	No
EGFR	7	+	55054199	55054221	GAGCTAGaCg	tcc	GGGCAGcCCC	No
EPHA2	1	—	16356670	16356692	CACCATGTTg	gcc	AGGCATGTCT	No
FANCC	9	—	97121069	97121098	GGACATGTTT	aaatacttga	GAGCTAtTTT	No
FAS	10	+	90741046	90741065	GGACAAGCCC		tGACAAGCCa	Yes
FDXR	17	—	70380716	70380735	GGGCAgGagC		GGGCTTGCCC	Yes
GADD45A	1	+	67925046	67925065	GAACATGTCT		AAGCATGCTg	Yes
GDF15_RE1	19	+	18357118	18357137	cAtCTTGCCC		AGACTTGTCT	Yes
GDF15_RE2	19	+	18357996	18358015	AGcCATGCCC		GGGCAAGaaC	Yes
GML	8	+	143894249	143894268	AtGCTTGCCC		AGGCATGTCC	Yes
GPX1	3	—	49370958	49370977	GGGCcAGaCC		AGACATGCCT	Yes
HTT/HD_RE1	4	+	3044349	3044371	cGcCATGTTg	gcc	AGGCTGGTCT	No
HTT/HD_RE2	4	+	3061438	3061464	AtGCTTGTTC	tacagaa	GAGCATGTTa	No
HTT/HD_RE3	4	+	3072173	3072198	GGGCcTGCTT	ccagtt	AAGCTTGCTT	No
HGF	7	—	81237693	81237712	AcACATGTaT		TTTCcTGTTT	No
HIC1	17	+	1905568	1905587	GGcgcTGCCC		TggCAcagCT	Yes
HSP90AB1	6	+	44322842	44322871	GGGAcTGTCT	gggtatcgga	AAGCAAGCCT	Yes
HSPA8	11	—	122437379	122437406	GcACTAGTTC	tggacctc	GcGCgTGCTT	Yes
IBRDC2	6	+	18495404	18495423	AGACAGGTCC		TGACAAGCAG	Yes
IER3	6	—	30820530	30820549	CCACATGCCT		CGACATGTGC	Yes
IGFBP3_RE1	7	—	45923287	45923306	GGGCAAGACC		TGCCAAGCCT	No
IGFBP3_RE2	7	—	45924206	45924226	AAACAAGCCA	c	CAACATGCTT	No
IRF5	7	+	128369513	128369534	AGGCATGCCa	ca	AGGCATGgTC	No
KRT8	12	—	51585038	51585059	ccGCcTGCCT	cc	ActCcTGCCT	No
LGALS3	14	+	54673996	54674020	GGGCTTGCAA	gctgg	AGCCTTGTTT	No
LIF	22	—	28971856	28971875	GGACATGTCG		GGACAGCTCC	Yes
LRDD	11	—	794414	794441	AGGCcTGCCT	gcgtgctg	GGACATGTCT	Yes
MAD1L1	7	—	2239405	2239424	ATTCAAGCTG		ATACTGAGTA	Yes
mdm2_RE1	12	+	67489008	67489027	AGTTAAGTCC		TGACTTGTCT	Yes
mdm2_RE2	12	+	67488970	67488989	GGTCAAGTTC		AGACACGTTC	Yes

MET	7	+	116099462	116099495	GGACggacag	cacgcgaggcagac	AGACAcGTgC	No
MLH1	3	+	37010251	37010271	AGGCATGTAC	a	GCGCATGCCC	Yes
MMP2	16	+	54068958	54068977	AGACAAGCCT		GAACTTGTCT	Yes
MSH2_RE1	2	+	47483388	47483420	AGGCTAGTTT	ttttttgttttc	AAGTTTCCTT	No
MSH2_RE2	2	+	47483593	47483613	GAcCTAGgCg	c	AGGCATGCgC	No
NDRG1	8	—	134379022	134379053	CCACATGCAC	acgcacgagcgc	GCACATGAAC	Yes
NLRC4	2	—	32344455	32344474	AGACATGTTC		CTGGTAGTTT	No
NOS3	7	+	150321654	150321676	GAGCcTcCCa	gcc	GGGCTTGTTC	No
ODC1_RE1	2	—	10505290	10505319	GGGCTcGCCT	tggtacagac	GAGCggGCCC	No
ODC1_RE2	2	—	10506214	10506238	GGACcAGTTC	caggc	GGGCgAGaCC	No
P2RXL1	22	+	19714729	19714750	GAACAAGggC	at	GAGCTTGTCT	No
P53AIP1	11	—	128316011	128316030	TCTCTTGCCC		GGGCTTGTCG	Yes
PCBP4_RE1	3	—	51971563	51971583	GgtCTTGgCC	c	AGACTTAGCa	No
PCBP4_RE2	3	—	51972515	51972544	GAACTTAAGA	ccgaggctct	GGACAAGTTG	No
PCNA	20	+	5048821	5048840	GAACAAGTCC		GGGCATaTgT	Yes
PERP	6	—	138466900	138466919	AGGCAAGCTC		CAGCTTGTTC	No
PLAGL1	6	—	144311857	144311876	CAACTAGACT		AGACTAGCTT	No
PLK2_RE1	5	—	57793125	57793147	GGtCATGaTT	cct	tAACTTGCCT	Yes
PLK2_RE2	5	—	57793858	57793877	AAACATGCCT		GGACTTGCCC	Yes
PLK2_RE3	5	—	57794080	57794102	AGACATGgTg	tgt	AAACTAGCTT	Yes
PLK3	1	+	45038183	45038208	TAACATGCCC	gggcaa	AAGCGAGCGC	Yes
PML	15	+	72074709	72074736	GcGCTgGCCT	ggagccag	GGGCATGTCC	Yes
PMS2	7	—	6012202	6012223	ATACTTGATT	tg	TTTCTTGTAA	No
PPM1J	1	—	113048062	113048081	GAACATGCCT		GAGCAAGCCC	Yes
PRDM1	6	+	106653151	106653170	GTGCAAGTCT		GGACATGTTT	Yes
PRKAB1	12	+	118590208	118590227	GTTCTTGCCG		CGGCTTGCCT	Yes
PTEN	10	+	89613057	89613090	GAGCAAGCCC	caggcagctacact	GGGCATGCTC	Yes
PYCARD	16	—	31121811	31121832	GTGCAAGCCC	ag	AGACAAGCAG	No
RABGGTA	14	—	23810330	23810357	CCTCTTGTGG	aacgtgca	AAGCCTGTCC	Yes
RB1	13	+	47775970	47775993	GGGCGTGCCC	cgac	GTGCgcGCgC	Yes
RFWD2	1	—	174445170	174445191	AGACTTGCCT	gt	GAACAGTCAC	No
RPS27L	15	—	61236487	61236506	GGGCATGTAG		TGACTTGCCC	Yes
RRM2B	8	—	103318244	103318263	tGACATGCCC		AGGCATGTCT	Yes
S100A2	1	—	151806761	151806780	GGGCATGTgT		GGGCAcGTTC	Yes
SCARA3	8	+	27564569	27564588	GGGCAAGCCC		AGACAAGTTg	Yes
SCD	10	+	102096562	102096582	GGGCcgGTCC	t	GGGCTAGgCT	Yes
SCN3B_RE1	11	—	123016908	123016927	TGGCAAGGCT		GAGCTAGTTC	No
SCN3B_RE2	11	—	123039640	123039659	TGACTTGCTC		TGCCTTGCCT	No
SERPINB5	18	+	59294974	59294994	GAACATGTTg	g	AGGCcTtTTg	Yes
SERPINE1	7	+	100556945	100556964	AcACATGCCT		cAGCAAGTCC	Yes
SESN1	6	—	109436914	109436933	GGACAAGTCT		CCACAAGTCa	Yes
SFN	1	+	27060408	27060427	GCATTAGCCC		AGACATGTCC	Yes

SH2D1A_RE1	X	+	123305989	123306014	TGGCTGGCTC	agctgt	CAGCTTGCTT	No
SH2D1A_RE2	X	+	123305980	123305999	GGGCTGGCTC		GGCTGGCTCA	No
SH2D1A_RE3	X	+	123305966	123305989	AACACTGCAC	tagt	GGGCTGGCTC	No
SLC38A2	12	+	45037706	45037735	AAcCATGCTg	ttacacgcac	CAGCTTGTCC	No
STEAP3	2	+	119719078	119719099	AGACAAGCAT	ag	GGACATGCTC	No
TAP1	6	—	32929058	32929083	GGGCTTGgCC	ctgccg	GGACTTGCCT	No
TGFA	2	—	70634503	70634522	GGGCAGGCCC		TGCCTAGTCT	No
TNFRSF10A	8	—	23138086	23138105	GGGCATGTCC		GGGCAgGagg	Yes
TNFRSF10B	8	—	22982080	22982099	GGGCATGTCC		GGGCAAGaCg	Yes
TNFRSF10C	8	+	23016747	23016766	GGGCATGTCC		GGGCAGGACG	Yes
TNFRSF10D	8	—	23077115	23077134	GGGCATGTCT		GGGCAGGACG	Yes
TP53	17	—	7531635	7531654	TTACTTGCCC		TTACTTGTCA	Yes
TP53INP1	8	—	96020186	96020205	GAACTTGggg		GAACATGTTT	No
TP63	3	+	190989527	190989549	TAACTTGTTA	ttg	AAACATGCTC	No
TP73_RE1	1	+	3556358	3556385	GtACTTGCCg	tccgggga	GAACTTGCag	Yes
TP73_RE2	1	+	3556376	3556406	GAACTTGCag	agtaagctgga	GAGCTTGaaT	Yes
TP73_RE3	1	+	3597020	3597050	GGGCAAGCTg	aggcctgcccc	GGACTTGGAT	Yes
TRIAP1	12	+	119368523	119368542	CTTCATGTCC		GTGCATGCCT	Yes
TRIM22	11	+	5668357	5668376	TGACATGTCT		AGGCATGTAG	Yes
TRPM2_RE1	21	+	44595747	44595771	GGCCTTGCCT	tgctc	AGGCCTGCTT	No
TRPM2_RE2	21	+	44596120	44596152	GAGCAGGTCT	gacctgcttccca	GGGCCTGCTT	No
TRPM2_RE3	21	+	44595752	44595771	TGCCTTGCTC		AGGCCTGCTT	No
TSC2_RE1	16	+	2041179	2041198	GGGCATGGTG		GCACATGCCT	No
TSC2_RE2	16	+	2042521	2042553	AGGCTAGTCT	gaaactcctgggc	TGACGTGACC	No
TSC2_RE3	16	+	2052179	2052199	TAACAAGCTC	g	GGGCTAGCCC	No
TYRP1_1	9	+	12683326	12683349	CGCCTAGTTT	gggt	GAGCAGATTT	No
TYRP1_2	9	+	12683340	12683372	GAGCAGATTT	gggattaattatc	AGGCAGCAAT	No
TYRP1_3	9	+	12683373	12683392	CCACATGCAC		TTAACAGTTC	No
TYRP1_4	9	+	12683314	12683335	AGACCAGCCC	cc	CGCCTAGTTT	No
TYRP1_5	9	+	12683363	12683382	AGGCAGCAAT		CCACATGCAC	No
UBD	6	—	29635901	29635920	AGGCATGCTC		AGTGGCGTGG	No
VCAN	5	+	82804022	82804042	AGACTTGCCA	c	AGACAAGTCC	Yes
VDR_RE1	12	—	46580342	46580361	TAACTAGTTT		GAACAAGTTG	No
VDR_RE2	12	—	46580352	46580374	AGGTTAGATG	tac	TAACTAGTTT	No

Table A-1: The 154 experimentally validated p53 response elements (REs) collected from Riley et al. [18].